Laser and Particle Beams (2001), *19*, 465–479. Printed in the USA.

Investigation of fast *z* pinches and hot plasma points

VASILIY I. AFONIN

Russian Federal Nuclear Center—Russian Research Institute of Technical Physics, POB 245, Snezhinsk, Chelyabinsk reg., Russia, 456770

(Received 22 May 2000; Accepted 25 March 2001)

Abstract

As a basis for this review the results of the investigations of a number of processes occurring at different stages of the fast *z*-pinch evolution, beginning with the electric explosion of a wire and ending with hot spot formation, have been assumed. At the same time the experimental results whose significant part had been obtained when investigating the explosion of thin aluminum and composite (W-Al-W; W-SiO_2-W) wires at the high-current SIGNAL accelerator (~220-kA current, ~50-ns rise time) have been used.

1. INTRODUCTION

Although detailed studies of fast *z* pinches have been carried out for many years, many problems of their physics remain unclear. The following can be given as examples.

A number of researchers (Aivasov *et al.*, 1985, Aranchuk *et al.*, 1986; Bobrova *et al.*, 1988; Ivanenkov *et al.*, 1995; Sarkisov *et al.*, 1995) have demonstrated that the initial stage of a wire explosion plays an important role in the plasma implosion and stagnation and influences the final parameters of the plasma in the *z* pinches. In particular, it was shown that, in a *z* pinch, there can exist an equilibrium, heterogeneous state with a cold dense core and a hot low-density corona, produced by a small fraction of the wire mass. Detection of a link between the parameters of a wire and current impulse, on one hand, and the parameters of the core and the corona of the pinch, on the other hand, is obviously important. This task is associated with the experiments about the creation of a plasma sheath with controlled parameters, which will be formed at the explosion of the multiwire cylindrical array and which is perspective for the objectives of inertial thermonuclear fusion (Lindl, 1995).

A number of papers (Branitsky *et al.*, 1991, 1999) describe experiments on gas liner implosions at the installation, ANGARA—5-1, in which both axial and azimuthal inhomogeneities of plasma were observed on the liner surface essentially just after its electrical breakdown. Although it was proposed (Kadomtsev, 1963; Velikov *et al.*, 1972) that the overheated (overheated and ionization) instability of pulsed gas discharge could be developed at the initial stage of high-current discharges in a gas-puff *z* pinch, leading to the skin layer splitting into current filaments, the questions of the mechanisms needed to form these inhomogeneities and their roles in the pinch evolution remained unsolved.

Hard X-radiation (XR) and ions with energies of approximately megaelectron volts were detected in pinches back in the 1950s. The explanation of these phenomena is reduced to the acceleration of particles in induction electric fields arising at quick breaking of constrictions (current necks) and to gas-dynamic acceleration (Zhdanov & Trubnikov, 1986). According to Yan'kov (1991), the situation may be different because of the mechanisms stabilizing the development of constrictions (current shunting through the corona, trapping of line radiation, etc.), although the noted effects still take place.

The hot plasma points (HPPs) in the pinch represent dense, nonstationary, high-temperature objects strongly radiating in the range of soft XR. The model of the radiative compression of the pinch (Koshelev *et al.*, 1991) shows that the equilibrium state of HPP is reached when the mode of radiation changes from a volume radiator to a surface radiator. However, this model simply does not take into account the influences of a shell structure of ions on the value of the critical current (being an analogue of the Pease-Braginskii current) and on HPP parameters. The question of the possibility for the HPP quasi-equilibrium mode in an optically thin plasma has remained beyond the capability of the model. The reasons for HPP concentration in the near-cathode part of a *z* pinch and HPP migration along its axis are also not clear (Aranchuk *et al.*, 1986; Bartnik *et al.*, 1990; Bartnik *et al.*, 1991).

Address correspondence and reprint requests to: Vasiliy I. Afonin, Russian Federal Nuclear Center, Russian Research Institute of Technical Physics, POB 245, Snezhinsk, Chelyabinsk reg., Russia, 456770. E-mail: afonin@five.ch70.chel.su

Sarkisov *et al.* (1995) present the results of the experimental investigation of the magnetic field structures in *z*-pinch plasmas. These data give evidence of switching the current from the constriction (or current neck) to the pinch periphery (corona), the availability of reverse currents, radial plasma ejection, and magnetic fields with pressures exceeding that conforming to the total current through the pinch. The interpretation of these effects within the framework of electronic MHD appears to be fragmentary and insufficiently convincing (Sarkisov *et al.*, 1995). In experiments on the compression of double liners (Branitsky *et al.*, 1999), as a possible reason for raising the reverse or countercurrents at the external boundary of the internal liner, the spontaneous magnetic fields (SMF) being generated in its corona by noncollinear gradients of plasma temperature and plasma density are proposed. However, the appearance of noncollinear gradients is not clear.

For the last few years the needs for X-ray microlithography explain the additional interest in laser-plasma and pinch sources of XR due to their high intensity and low cost. But a *z* pinch is an extended linear object, in which HPPs are located rather chaotically, and without spatial localization of HPP, a pinch is of little use for these applied purposes. In Aranchuk *et al.* (1997) and Gus'kov *et al.* (1998), spatial localization of HPP is achieved by introducing a perturbation into the initial geometry of the load. Are there other ways to obtain this result?

The results of investigations on these problems and phenomena of the fast *z*-pinch physics, which cover the main stages of its evolution, beginning with the electric explosion of the wire and ending with the HPP formation, were used as the basis of this review. In this review, experimental results are used that were obtained during the investigation of the explosion of thin aluminum and composite (W-Al-W; W-SiO_2-W) wires on the high-current SIGNAL accelerator (Afonin *et al.*, 1988*b*) with an inductive energy storage and an opening plasma switch (300-kV voltage pulse, a load current ~200 kA and rise time of ~50 ns). The diagnostic complex of the installation included a multiframe X-ray photorecorder, optical and X-ray streak-cameras, spectrographs, pinholes, and so forth (Afonin *et al.*, 1988*a*, 1996, 1997*a*, *b*, 1999).

2. PINCH CORONA FORMATION

The main physical processes occurring during the electrical explosion of a thin (20–40 μm in diameter) aluminum wire under the action of a voltage pulse with a triangular shape with 0.3- to 3-MV maximum and 10- to 50-ns rise time are described by Afonin (1999).

According to the simplest transition model, ignoring the substance motion and heating inhomogeneity, when reaching a temperature $T \sim 2$ eV in aluminum, a nonequilibrium metal–plasma transition takes place. As a result, a dense (6×10^{22} cm^{-3}) and cold (~2 eV) plasma is formed with an average charge of ions $Z \sim 1$. Under the action of high pressure, the plasma expands into the vacuum. The plasma is initially cooled adiabatically and then heated under conditions of Joule heating when Joule heating dominates the adiabatic cooling. The process of the wire explosion and the formation of the current shell requires a comparatively long interval of time and is characterized by the slow rise of current in a pinch. Estimates show (Afonin, 1999), that at $dE/dt = 3 \times 10^{13}$ V/s-cm, at $t \sim 13$ ns, a current shell is formed having a temperature of $T \sim 2.3$ eV, an ion density $N \sim 9 \times 10^{20}$ cm^{-3}, whose thickness $\delta \sim 80$ μm is comparable with its radius r and, through which ~3 kA current is flowing. At $dE/dt = 0.6 \times 10^{13}$ V/cm-s the sheath is formed by $t \sim 30$ ns, at the same time $\delta \sim r \sim 120$ μm, $T \sim 1.6$ eV, and $N \sim 4.2 \times 10^{20}$ cm^{-3}. Measurements of the current-driven explosion of thicker wires demonstrated current shell formation at later times with higher ion densities.

With further plasma heating, the skin layer thickness continues to decrease, the plasma radius increases, and the plasma density decreases monotonically. With increasing current, the skin layer plasma is decelerated by the magnetic field, and it is possible to attain a shell quasi-equilibrium with pressure of the magnetic field current J(A) flowing in plasma.

For a homogeneous plasma shell (corona), whose thickness is δ (cm), radius is R (cm), temperature is T (eV) and ion density N (cm^{-3}) with the average charge Z, the possible quasi-equilibrium parameters are determined from the Bennett condition and the balance of Joule heating, radiative losses from surface of the optically thin plasma, the conservation of mass, and Ohm's law. This has the form of $\delta = 0.097(\exp(x)/x)^{0.5}/T^{5/4}$, $N = 2.66 \times 10^{10} \times T^{1.5}J_1^2/Z\exp(x)$, $R = 1.5 \times 10^6(\exp(x)/x)^{0.5}Z^{0.5}R_0/T^{0.5}J_1$, $E_1 = J/2\pi R\delta\sigma$ (V/cm), where E_1 is the intensity of the field in plasma, $J_1 = 2.7 \times 10^5(\Lambda/k)^{0.5}/2^{0.5}$ is the critical current in the solid plasma cylinder that is connected with the conforming critical current J in the shell by the relationship $J = J_1R/2\delta$, $\sigma = 30T^{3/2}/Z$ is the unmagnetized conductivity of plasma, $k = 1 + U_{Z-1}/T + 1.7 \times 10^7\exp(-\Delta E/T)m_n/Z^2T$ is the radiation factor, R_0 is the initial radius of wire, U_Z is the ionization potential, $\Lambda = 10$ is the Coulomb logarithm. The excitation energy ΔE of ion with its charge Z can be estimated from the expression $\Delta E = (2n+1)U_Z/(n+1)^2$, where $n = 1, 2, 3$ for the transitions to *K*-, *L*-, *M*-shell, but the average charge value Z is from the usual relations for the plasma coronal equilibrium. The expression for the critical current J_1 has been obtained from the equality of Joule heating power of the homogeneous plasma column to its volume radiative losses. The radiative factor takes into account the contribution from the line and recombination radiation to the radiative energy losses of the optically thin plasma. The estimation of the line radiation power was obtained from the semi-empirical relationship (Vainstein *et al.*, 1979) for the excitement velocity, being averaged over Maxwell distribution, of the optically resolved transition $\langle\sigma^{10,11}v\rangle = 32 \times 10^{-8}f_{10,11}(\mathrm{Ry}/\Delta E)^{3/2}\beta^{1/2}e^{-\beta}p(\beta)$, where l_0, l_1 are orbital quantum numbers, s is the electron spin,

https://doi.org/10.1017/S0263034601193018 Published online by Cambridge University Press

$f_{10,11}$ is the oscillator force of the transition $l_0 \rightarrow l_1$, Ry is the Rydberg constant, $\beta = \Delta E/T$, $p(\beta)$ is the multiplier ($p(\beta) \approx 0.2$ for $\beta \geq 1$).

The estimates of parameters of the corona produced in the explosion of an aluminum wire 20 μm in diameter for various temperatures T (eV) are listed in Table 1 (δ and R are expressed in microns, J in kiloamperes, E_1 in kilovolts per centimeter, and N in 10^{18} cm^{-3}).

We assume that, during heating and expansion of the plasma shell and its deceleration by the magnetic field produced by the increasing current at $dE/dt = (0.6–3.0) \times 10^{13}$ V/s-cm, the thickness and density of the shell decrease monotonically from those corresponding to $\delta = 80–120$ μm, $N = (4.2–9) \times 10^{20}$ cm^{-3} (at $t = 12–32$ ns when the current sheath is formed and the field is $E = 240–190$ kV/cm) to those corresponding to quasi-equilibrium. From the data presented in Table 1, we can infer that quasi-equilibrium can occur at $J = 176$ kA, $\delta = 32$ μm, $R = 450$ μm, $T = 65$ eV, $N = 2.9 \times 10^{19}$ cm^{-3}, and the field $E = 100$ kV/cm. Further evolution of the plasma depends on the capabilities of the accelerator. If the accelerator voltage decreases, compared to that being necessary for quasi-equilibrium, then the plasma expands. When the current in the corona exceeds its quasi-equilibrium value, it is possible to expect its collapse. It is easy to see that, with a diode-voltage rise time of $\tau = 10$ ns, both the time of the shell formation, $t = 12$ ns, and the time during which quasi-equilibrium is established, $t = 16.7$ ns (which corresponds to 100 kV/cm), fall into the time period in which the current generator voltage is decreasing. Both the voltage and current decrease with time. The corresponding quasi-equilibrium radius and thickness of the corona increase, that is, it continues to expand. At $\tau = 50$ ns, the shell is formed only at $t = 30$ ns, when $E = 190$ kV/cm. Analogous to the above discussion, we conclude that quasi-equilibrium is reached at $R = 280$ μm, $\delta = 20$ μm, $T = 80$ eV, $J = 210$ kA, $E = 220$ kV/cm. It occurs at the time $t = 37$ ns. The field and the current continue to increase with time, which results in further heating and compression of the corona. Taking into account the absence of counteracting pressure in the corona plasma, it is possible to expect it pinching onto the cold core plasma. We can also expect that the corona will expand and cool when the field starts to decrease. Thus, when the current rise time is short enough (10 ns), the formation of the corona is followed by its expansion in the outer space. When the rise time is long (50 ns), the formation of the corona can be accompanied by its pinching onto the axes.

Table 1. *Quasi-equilibrium parameters of the pinch plasma corona.*

T	30	36	40	50	65	80	100	200
Z	6	7	7	8	8	9	10	11
δ	120	210	50	80	32	22	13	70
R	2800	1800	1400	850	450	282	130	290
N	0.57	4.74	3	8.44	29	82	1.37	71.3
J	104	123	130	144	176	210	250	370
E_1	5.9	5.5	27	26.2	101	222	784	37.6

It is easy to note that at $T = 40–65$ eV the corona contains 7–14% of the initial mass of the wire. Moreover, from the relationships for the parameters of quasi-equilibrium, it is seen that with an increase in the initial radius of the wire, the values of the radius and the quasi-equilibrium current proportionally increase at invariable thickness of the corona and density of plasma, that leads to the proportional decrease in the wire mass transferring into the corona plasma. For example, if the initial wire diameter is 40 μm, then less than 4% of its mass is converted into the plasma corona. All this correlates with the results described earlier (Aivasov *et al.*, 1985; Bobrova *et al.*, 1988; Kalantar & Hammer, 1993).

3. IONIZATION–THERMAL INSTABILITY OF THE CORONA

Thus, thickness, temperature, and density of the corona plasma do not depend on the initial radius of the wire, whereas its radius and value of the quasi-equilibrium current are directly proportional to it. As a consequence of this, at the electric explosion of the wire, the radial perturbations of its surface can be transformed into the radial perturbations of the corona surface, which contribute to the evolution of the MHD instability of the sausage type.

But the initial perturbations of the corona can be formed in that case when in the initial wire there are inhomogeneities associated with crystalline structure of metal, inclusion of impurities, and so forth. These inhomogeneities can lead to the formation of initial perturbations in the form of perturbations in temperature and electron density of the corona plasma, which also contribute to the evolution of sausage type instabilities.

According to Raizer (1987) and Afonin (2001) the initially homogeneous, nonisothermal, and ionization equilibrium plasma consisting of multicharged ions of stationary electric discharge supported by a constant electric field may be unstable relative to longitudinal and axial perturbations of its electron temperature and/or its electron density. The magnitude of the instability can be found from the analysis of the linearized equations of balance of electron energy in stationary, nonviscous, nonisothermal, and nonradiating plasma of multicharged ions and equations of its kinetics, into which the ionization by electron impact, photo- and three-particle recombination are included. At the same time, as the estimates (Afonin, 2001) show, the characteristic time of the ionization–thermal instability development in the pinch corona plasma amounts to ~1 ns. At the instability evolution, the plasma transfers to the spatially inhomogeneous state: Azimuthal and axial inhomogeneities appear in it in the form of plasma filaments and strata, respectively. For example, in Figure 1 (Branitsky *et al.*, 1999), a laser shadowgraph of an argon jet which was obtained in the experi-

https://doi.org/10.1017/S0263034601193018 Published online by Cambridge University Press

Fig. 1. Laser shadowgraph of an argon jet from the conic nozzle with the cathode cut diameter of 30 mm at the discharge current ~1 MA prior to the compression beginning. Azimuthal and axial inhomogeneities of plasma being present in the layer of current are also seen. Light area: plasma.

ment at the installation "Angara—5-1" is given where filaments and strata are seen.

For the evolution of the azimuthal ionization–thermal instability as well as in case of the volume gas discharge contraction (Raizer, 1987), it is first necessary for the electrons to be born in the region of their increased density and, secondly, they should die in same region not far from where they are born. Otherwise the initial perturbation attenuates because of electron diffusion. Proceeding from this, the characteristic transverse size of filament $D_R \sim \lambda/2$, where λ is the perturbation wavelength, can be determined as double the distance at which an electron diffusing in electron–ion collisions is displaced during its lifetime being equal to the characteristic time of recombination $\tau \sim (C_Z^r N)^{-1}$, where C_Z^r is the recombination rate of ions with a mean charge Z and ion density N. According to Braginsky (1963), the directed velocity $\vec{V}$ of electrons with density N_e relative to ions can be found by means of the quasi-stationary equation of motion of plasma ions in the electric field E under condition of equality to zero of its pressure gradient in the form of $ZeNE - en_e k_1 \vec{j}/\sigma_\perp + k_2 N_e k_0 \nabla T_e = 0$, where $k_0 = 1.6 \times 10^{-12}$ erg/eV, $k_1(Z)$ is the numerical factor ($k_1 = 0.29$ when $Z \gg 4$), $k_2(Z)$ is the numerical factor ($k_2 = 1.5$ when $Z \gg 4$), $\sigma_\perp = 0.9 \times 10^{13} T^{3/2}/(\Lambda/10)Z$ is the plasma conductivity, j is the current density, Λ is the Coulomb logarithm ($\Lambda = 10$). Then, by using Einstein's formula for the average square of the electron displacement in the plane being perpendicular to the filament axes, it is possible to obtain

$$D_R \sim 5.27 \times 10^{-14} (A/\rho Z) T_e^{1.25}/(k_1 C_Z^r)^{0.5}, \quad (1)$$

where A is the atomic weight of element, T_e (eV) is the electron temperature, ρ (g/cm^3) is the plasma density.

From Raizer (1987) the characteristic spatial scale of strata can be determined in which the electric field and electron temperature decrease in the region with increased density of electrons and vice versa. As a consequence of this, in the regions with increased electron density, the ionization rate decreases and the recombination rate increases; as a result, the density fluctuation can attenuate or, on the contrary, can develop depending on the electron temperature relaxation length D in the field E which, according to Raizer (1987), has the form $D = 0.8L/\delta^{0.5}$, where L is the electron pass length; $\delta \sim m_e/m_I$ is the energy share transferred to the ion by the electron each collision; m_e and m_I are the mass of electron and ion, respectively. Just at the length D, the electron temperature begins to conform to the field E. At the perturbation half-wave of $\lambda/2 < D$, electron temperature fails to drop to the value conforming to the decreased field. In case of $\lambda/2 > D$, temperature succeeds in following the behavior of the field E and the perturbation attenuates. Proceeding from this, let us take the value of D as an upper boundary of the characteristic linear size of strata. Insofar as $L = v\tau_{ei}$, where $v = 6.7 \times 10^7 T_e^{0.5}$ is the thermal velocity of electron, $\tau_{\rm ei} = 3.15 \times 10^8 A\delta T_e^{1.5}/NZ^2$ is the electron–ion collisions frequency (Raizer, 1987), then

$$D = 4 \times 10^{14} A^{0.5} T_e^2/NZ^2. \quad (2)$$

It should be noted that in formulas (1) and (2), the temperature, density, and charge of ions refer to the unperturbed plasma.

Thus, at the development of ionization–thermal instability the pinch periphery plasma is divided into longitudinal filaments and transverse strata with the characteristic size D_R and D, respectively, in which plasma density and temperature are increased as compared to their average equilibrium values. Both the strata and filaments are distant from each other by plasma regions of the same scales, but with decreased density and temperature. In stratified filaments, maximum values of plasma density fall within the filament axes, unperturbed ones conform to the filament boundaries and strata boundaries. At the same time, as has been noted above, the electron temperature distribution is sheared at the distance $\sim D/2$ relative to the electron density distribution in strata plasma. All this can stipulate nonparallel gradients being necessary for the magnetic fields generation in conformity with equation

$$\partial \vec{H}/\partial t = 10^8 (\nabla N_e \times \nabla T_e)/ZN_e \quad (\text{G/s}). \quad (3)$$

4. COUNTERCURRENT AT *Z*-PINCHES BOUNDARY

Let us estimate the experimental data (Sarkisov *et al.*, 1995; Branitsky *et al.*, 1999), while noting that it is possible to use the value D_R as a characteristic length of change in plasma density from minimum (in the interfilamentary interval) to maximum (in the filament center). Analogously, the half-wavelength D can serve as characteristic length of the plasma temperature change.

Figure 2 (Sarkisov *et al.*, 1995) presents radial distributions of the magnetic field, electron density, strength, and density of current in the cross section of the pinch being formed under explosion of Ta wire, 20 μm in diameter, at high-current generator GAEL. They were obtained within 30 ns after the beginning of current when its strength amounted to 55 kA, but the instability mode $m = 0$ did not yet succeed in being developed.

https://doi.org/10.1017/S0263034601193018 Published online by Cambridge University Press

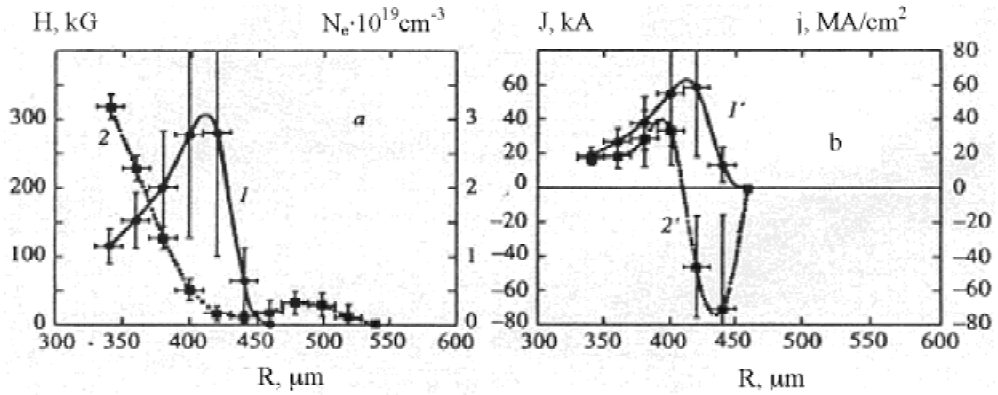

Fig. 2. (a) Radial distribution of magnetic field induction (1) and electron density (2); (b) radial distribution of current strength (1′) and current density (2′).

In Figure 2a it is possible to note the equality of scales (~50 μm) of countercurrent zones and the perturbations of electron density at its mean value 2.5×10^{18} cm^{-3}. The magnetic field induction reaches its maximum ~300 kG at $R \sim 410$ μm, after which it quickly drops to zero at $R \sim 470$ μm.

Supposing that the perturbation in electron density is induced by instability, the characteristic scale of filaments and strata is estimated. By using the expressions (Derzhiev *et al.*, 1986; Zel'dovich & Raizer, 1967)

$$C_Z^i = 5.3 \times 10^{-8} (\mathrm{Ry}/T_e)^{1.5} \cdot (\xi/x \cdot \exp(x)) \times \{\ln[(1+x)/x] - 0.4/(1+x)^2]\}, \quad (4)$$

$$C_Z^r = 8.75 \times 10^{-27} Z^3 N_e / T_e^{4.5} \quad (5)$$

for velocities of ionization by electron impact and the triple recombination, it is easy to verify that $C_Z^i \sim C_Z^r \sim 3.4 \times 10^{-10}$ cm^3/s at $N_e = 2.5 \times 10^{18}$ cm^{-3}, $T_e = 4$ eV, $U_Z = 23$ eV, and $Z = 2$ (ξ is the number of equivalent electrons in the external shell of Z ion, $x = U_Z/T_e$). The estimate from formula (1) leads to $D_R \sim 60$ μm that agrees well with the experimental value. In its turn, the estimate (2) of strata sizes D leads to the value $D \sim 170$ μm. Assuming that pressure in plasma is constant, one obtains maximum $T_e =$ 6 eV, minimum $T_e = 2$ eV. By using these data as characteristic values, from (3) it is possible to obtain the estimation of the field intensity $H \sim 1.4 \times 10^5$ G and rise time $\tau = 30$ ns that is less by a factor of two than the measured value.

Let us refer to the data of the experiment at the installation "Angara—5-1" that was performed to study the shells' interactions in a two-stage scheme (Branitsky *et al.*, 1999). According to this, just before the impact of the external xenon shell with the current layer, whose thickness $d =$ 1 mm, against the internal one (shunt), at the latter, the countercurrent equal to ~30 kA was registered. (The shell length amounted to 1 cm, rate of its converging $V \sim 4 \times 10^7$ cm/s, the shunt radius $R = 0.25$ cm, and the shunt resistance $B = 5 \times 10^{-3}$ Ω.) For explaining this phenomenon we make use of data of similar experiments (Branitsky *et al.*, 1991, 1999), according to which, just after the disruption of the xenon liner, small-scale inhomogeneities arise along the liner axis in the form of "ripples", 1–2 mm in diameter. Subsequently, dense plasma filaments, 1–3 mm in diameter, parallel to the liner axis occurred. The initial concentration of the xenon liner atoms amounted to 2×10^{17} cm^{-3}, the average charge of the ions beyond plasma perturbations was $Z = 3$–5.

For simplicity, we assume that beyond the perturbations the plasma is in ionization equilibrium, at the same time the density of ions with charge $Z = 3$ is equal to the xenon atom density. Noting that at $T_e < 18$ eV, three-particle recombination prevails over the photorecombination and equating (4) and (5), it is easy to find $x \sim 6.6$; $T_e \sim 7$ eV; $C_Z^i \sim C_Z^r \sim 2 \times 10^{-11}$ cm^3/s. Then $D_R \sim 0.2$ cm, $D \sim 0.12$ cm, which is in good agreement with experiment. With heating, the plasma perturbations are "spreading." Indeed, if $Z = 5$, then at $T_e <$ 25 eV, the three-particle recombination prevails and then $C_Z^i \sim C_Z^r \sim 10^{-11}$ cm^3/s at $T_e = 13$ eV, $x = 6.1$. At the same time $D_R \sim 0.4$ cm, $D \sim 0.15$ cm. Hence we conclude that in the liner plasma, as it is heated and compressed, azimuthal inhomogeneities essentially disappear; however, the axial ones are preserved (Branitsky *et al.*, 1991, 1999). In accordance with this, we assume $T_e = 13$ eV, $Z = 5$, $D = 0.15$ cm, $d = 0.1$ cm, and estimate SMF in the coordinate system associated with plasma. For this we consider the part of the shell schematically presented in Figure 3 where the coordinate Y_0 conforms to temperature maximum in stratum, the coordinates $Y_0 \pm D$ to minimum; and plasma density maximum corresponds to R_0.

When choosing the characteristic time τ of the SMF generation, we take into account that equation (3) is written disregarding the magnetic field diffusion. Therefore, when time τ is equal to the characteristic time of the magnetic field diffusion $\tau_1 \sim 4\pi\sigma(d/2)^2/c^2$, where c is the velocity of light, $\sigma = \sigma_\perp/k_1$, it is possible to expect the SMF saturation. For the shown parameters of the shell plasma $\tau_1 \sim 8$ ns.

https://doi.org/10.1017/S0263034601193018 Published online by Cambridge University Press

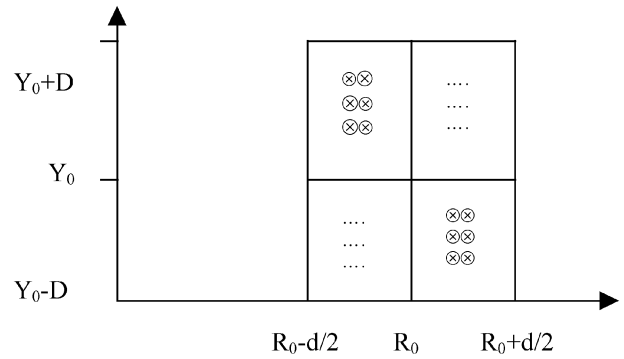

Fig. 3. Schematic view of the stratified shell part and the spontaneous magnetic field direction: direction "to us" is shown by points, "from us" by small circles with a cross.

Then at perpendicular gradients the estimate of the solenoidal SMF intensity leads to the value $H \sim 280$ G. By using the Maxwell equation $\oint \vec{E} d\vec{L} = -(1/c) \int (\partial \vec{H}/\partial t) d\vec{S}$, one will obtain the value of the induction electric field $E \sim (d/8c)\partial H/\partial t$; if L is the circuit with radius $d/4$, field H does not depend on the radial coordinate. The transition into the laboratory coordinate system that moves relative to the reference system associated with the shell plasma leads to $E_1 \sim (d/8c)\partial H/\partial t + (1/c)VH \sim (1/c)VH$. The field E_1 excites the shunt current $J\,(A) = 300E_1/B \sim 22$ kA. And, finally, from Figure 3 it is possible to note that if along the shell length the even number of half-waves D can be fitted in, then in the shunt induction currents will appear to be compensated. The negative current in the shunt can occur at the odd number of half-waves and/or at zipper effect.

Thus, the estimates of the characteristic scales of perturbations, inductive currents, and SMF intensities agree rather well with experimental data. As a result of this, the supposition that the reason of the countercurrent may be SMF is rather substantiated.

With regard to these conceptions, the gas-liner breakdown dynamics can be seen as follows. At the initial instant that the electric breakdown of a gas shell takes place along the separate channels, in which temperature and the degree of plasma ionization are increasing in accordance with the development of the ionization–overheated instability of the volume gas discharge (Velikhov *et al.*, 1972), when the atoms ionize and the triple recombination of ions being formed, mainly, takes place. The intense ultraviolet radiation going out of these channels is absorbed by the surrounding gas that leads to its volume ionization, flowing of current, and heating. With the appearance of multiply-charged ions, the ionization–thermal instability of plasma develops, which can be substituted (prior to opening the next ion shell) by the overheated instability (Kadomtsev, 1963). As a consequence of the instability, a stratification and a filamentation of the plasma take place. With the shock wave arrival when $T_I \geq T_e$ is set up, the given instability attenuates and both the Rayleigh–Taylor instability of plasma under axial perturbations of temperature (Vikharev *et al.*, 1990) and the azimuthal instability under nonisothermal mode of the liner acceleration (Vikharev *et al.*, 1990; Branitsky *et al.*, 1991) develop.

5. MHD INSTABILITY

According to Section 3, in the corona plasma the ionization–thermal instability is possible. Perturbations in electron density and temperature of plasma can be initial ones for the MHD instability evolution. For studying this phenomenon at the installation SIGNAL, a series of experiments on the explosion of thin aluminum wires has been performed (Afonin *et al.*, 1997*b*). The visible photochronogram of the pinch evolution is shown in Figure 4. Figure 5 presents the pinch luminosity at different instants.

It is seen that already at the initial stage of the wire explosion a small-scale inhomogeneity of the pinch luminosity exists. The scale length of the inhomogeneity increases with time up to $\lambda \sim 1.2$–1.5 mm. A typical X-ray photochronogram of the z pinch is presented in Figure 6.

It is seen from the photochronogram that, before the occurrence and subsequent evolution of HPPs, the character-

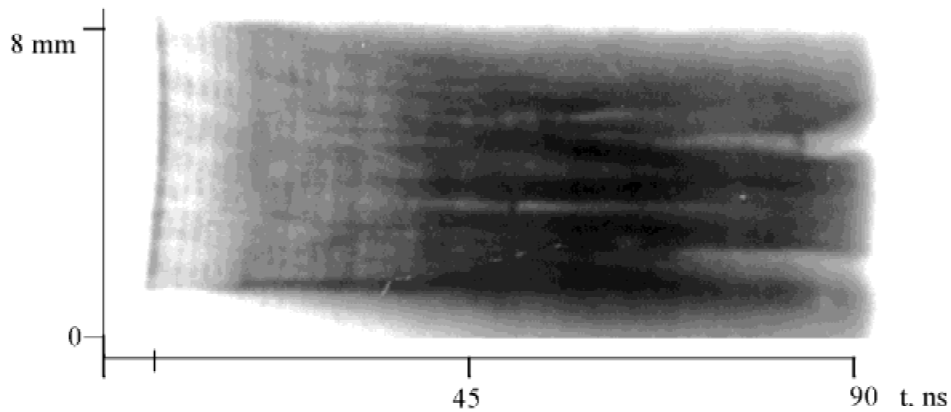

Fig. 4. Photochronogram of Al wire explosion in visible light.

https://doi.org/10.1017/S0263034601193018 Published online by Cambridge University Press

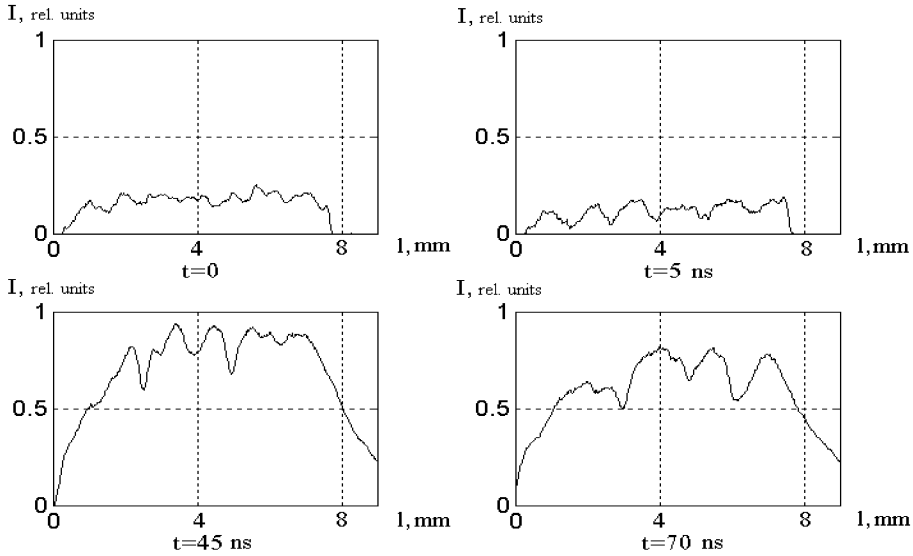

Fig. 5. Luminosity of the *z*-pinch plasma column (arb. units) at different instants.

istic scale-length of pinch inhomogeneity is 0.1–0.15 cm. The images, one of which is represented in Figure 7, were produced with an SKhR4 frame recorder (Afonin *et al.*, 1999). It shows the creation of corona initial perturbations with a wavelength ~1 mm.

According to Section 2, with the explosion of a 20-μm-diameter aluminum wire at the SIGNAL installation, it is possible to expect the formation of a corona with parameters $T \sim 50-65$ eV, $R \sim 0.09-0.05$ cm, $N \sim (0.8-3) \times 10^{19}$ cm^{-3}, $Z \sim 8$, $J \sim 144-176$ kA. Using these results and the concept of the onset of ionization–thermal instability in the multiply charged ion *z*-pinch plasma (Afonin, 1995, 2001), we can estimate the characteristic scale length of the perturbations. Actually, the condition for the onset of instability of this type is $K > 10^9 \rho \xi^{0.5} Z^{1.5} x_0/(AT^{2.5})$, where $K = 2\pi/\lambda$ is the wave number, A is the atomic weight, ξ is the number of equivalent electrons in the state with the principal quantum number n, ρ (g/cm^3) is the plasma density, $x_0 = U/T$, U is the ionization energy. From here, we obtain the estimate for the perturbation scale length $\lambda > 0.01$ cm at the beginning of the corona compression.

As the corona is compressed, the produced axial temperature perturbations can initiate MHD instabilities. From all the spectrum of initial perturbations with $\lambda > 0.01$ cm, only those for which $\lambda/2 \sim x \sim R$ (where x is the distance covered by the thermal or shock wave propagating in the radial direction) can develop into HPPs. For shorter wavelengths, due to thermal conductivity, the thermal waves will be overlapped at a large distance from the pinch axis, so that an almost cylindrical thermal shock wave arrives at the axis (core) of the system, and HPP is not formed. It can be concluded that HPPs are produced by perturbations whose $\lambda \sim 2R$. Consequently, the shock waves propagating along the thermal perturbations to the axis of the system can produce from 5 to 8 HPPs over the plasma column length $l =$ 0.8 cm, which agrees well with experimental results. The numerical modeling, which was carried out on the 2-D MHD-code MAG (Afonin *et al.*, 1996), also confirms the assumption that the MHD instability can arise from the temperature perturbations.

Thus, the experimental results and their analysis indicate a significant role of the ionization–thermal instability of *z*-pinch plasma in the mechanism of HPPs generation. It is possible to note, that according to Afonin (1995, 2001), the *z*-pinch strata represent a wave propagating in the longitudinal direction. This mechanism, probably, explains the enhanced concentration of initial perturbations in the vicinity of one of the accelerator electrodes, therefore, and the HPPs concentration near this electrode.

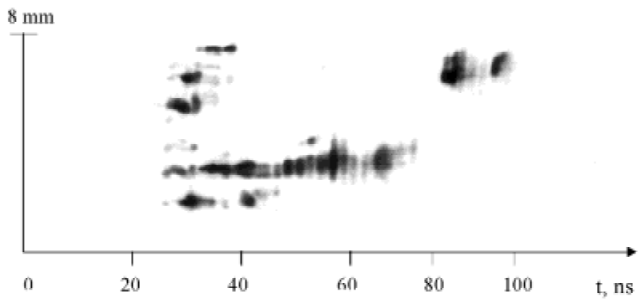

Fig. 6. X-ray photochronogram of the Al wire explosion.

6. VORTEX ELECTRIC FIELDS

Let us consider the processes occurring during the convergence of the constriction of the pinch current-carrying corona (Afonin, 2000). For simplicity, we will assume the constriction to be a hollow cylinder with the outer radius b, thickness δ, and length h; this cylinder moves from the radius R (R is the quasi-stationary corona radius) towards the

https://doi.org/10.1017/S0263034601193018 Published online by Cambridge University Press

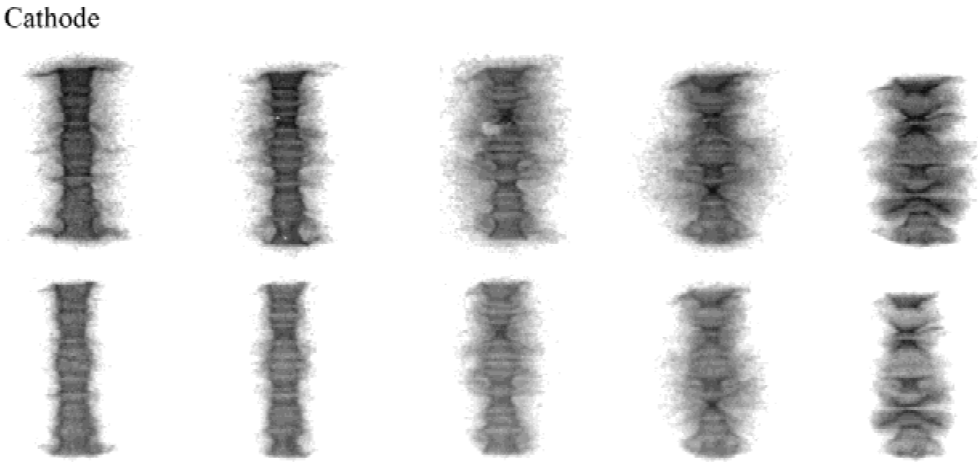

Fig. 7. Subsequent photodetector images: the diameter of the aperture of the SKhR4 pin-hole chamber is 35 μm for the upper row and 25 μm for the lower row, the frame exposure time is 12 ns, and the interval between frames is 10 ns; the first frame starts within 65 ns after the beginning of the load current pulse. The maximum current is 220 kA, the current rise time is 170 ns. The load is a 10-mm-long 44-μm-diameter aluminum wire.

pinch axis with the average velocity U under the action of the magnetic field pressure produced by the current J. Then, according to Faraday's Law, in the constriction cavity $b \leq r \leq R$, there is a vortex electric field with maximum $E(R,t) = -2 \times 10^{-9}(UJ/b)[2 - b/R + (2b/h)\ln(R/b)]$. The inertial drift of ions in crossed magnetic and varying electric field $dE/dt = -410 - 9J(U2/b2)(1 + b/h)$ leads to origin of the plasma jet. A jet drifting both in the radial and axial directions with velocity $V \sim 10^{-3}(AR^2U^2/Jb^2Z)(1 + b/h)$ will take the form of a radial plasma protuberance emerging from one of the ends of the constriction cavity and bent towards the other end (see Figures 8 and 9).

When one or more constrictions change the direction of motion, the characteristic bending of the jets toward the cathode can occur, which is clearly seen in the first upper and lower frames in Figure 9.

Thus already at another boundary of the constriction cavity, a second jet emerges, which propagates toward the cathode. The structure of two jets shunting the constriction is clearly seen in the first upper and lower frames in Figure 6.

At shunting, the current from the constriction is displaced into the region of jets. Moreover, when the current is intercepted by the jets, the acceleration of electrons takes place in the inductive electric field with the subsequent deceleration at the electrode of the accelerator that can lead to the appearance of hard X-radiation registered in a number of experiments, including those on the installation SIGNAL. Estimates (Afonin, 2000) show that, for example, for one of the corona quasi-equilibrium variants of Table 1 (R = 450 μm, J = 176 kA) the motion velocity of the constriction can reach 160 km/s with generating the field $E \sim 3.4$ MV/cm. The plasma jet shunts the constriction at its length $h \leq 1.8$ mm. At the same time the ions energy can reach 10 MeV, the electrons energy ~ 0.6 MeV.

7. HOT PLASMA POINTS

According to data (Afonin *et al.*, 1988*a*, 1996, 1997*a*) obtained in experiments at the installation SIGNAL on the explosion of thin (20- to 30-μm diameter) aluminum wires, the pinch corona diameter amounts to 140–500 μm, the transverse size of HPP is ~10–30 μm, the electron temperature is ~ 0.4–0.9 keV, the electron density is $\sim 10^{23}$ cm^{-3}, and the characteristic lifetime is of the order of nanoseconds.

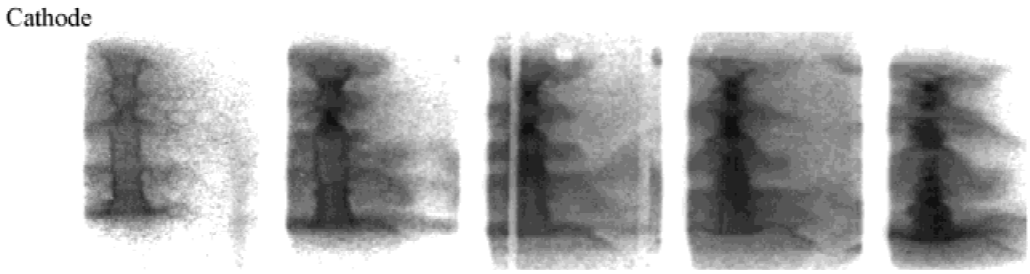

Fig. 8. Successive X-ray images of the load plasma column: the diameter of the aperture of the SKhR4 pin-hole camera is 100 μm, the frame exposure time is 12 ns, and the interval between frames is 10 ns; the first frame starts 75 ns after the beginning of the load current pulse. The load is aluminum wire 20 μm in diameter and 8 mm in length; the maximum current is 190 kA, the current rise time is 150 ns.

https://doi.org/10.1017/S0263034601193018 Published online by Cambridge University Press

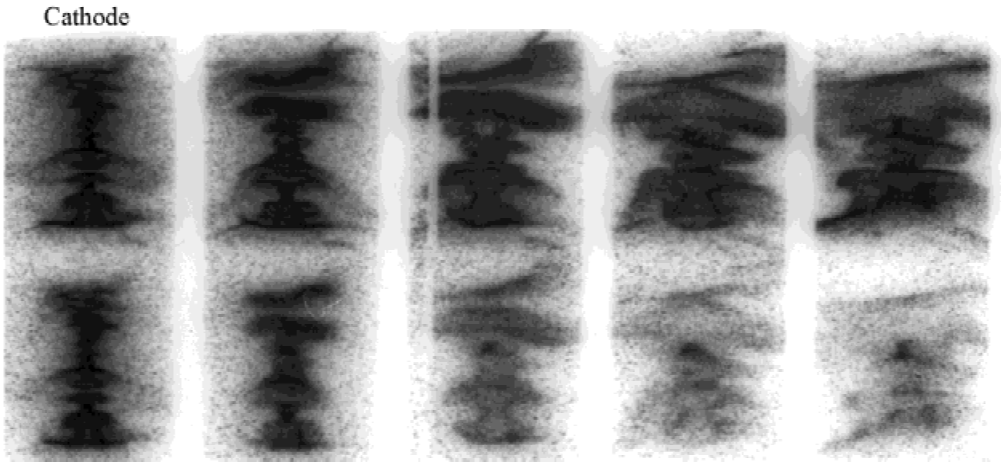

Fig. 9. Successive X-ray images of the load plasma column: the diameter of the aperture of the SKhR4 pin-hole chamber is 30 μm for the upper row and 10 μm for the lower row, the frame exposure time is 7 ns, and the interval between frames is 10 ns; the first frame starts 80 ns after the beginning of the load current pulse. The load is aluminum wire 20 μm in diameter and 8 mm in length; the maximum current is 150 kA, the current rise time is 80 ns.

The experimental data both on HPPs and micropinches (Koshelev *et al.*, 1991) can be interpreted almost entirely within the framework of the radiative compression model (Aglitskii *et al.*, 1991; Afonin, 1994; Afonin *et al.*, 1997*a*). At the plasma column compression, the plasma density increases in it as $1/r^2$. This leads to the growth of the optical thickness ($\sim 1/r$), partial absorption of radiation, additional heating, and plasma pressure growth. As a result, the plasma column transforms into the state of quasi-equilibrium with the magnetic field pressure under which the power of its Joule heating is compared with the rate of the energy loss through the radiation from the surface of the column being considered as an optically thin body. According to Afonin (1994), the expression for the radiation losses power of the optically thin plasma layer, d in thickness, has a form S (W/cm^2) $= 2dS_p/l$, where $S_p = \sigma T^4$ is the one-sided flow of equilibrium radiation, T is the temperature in electron volts, $\sigma = 1.03 \times 10^5$ W/cm^2-eV^4 is the Stefan–Boltzmann constant, l (cm) $= 3.03 \times 10^{15} T^2 \exp(x)/N_e Z x$ is the radiation mean free path in multiply-charged ion plasma, $x = U_z/T$, U_z is the ion ionization potential. In its derivation (Zel'dovich & Raizer, 1967), the expression used for the spectral brightness of a layer was in the form of $S_\nu = S_{\nu p}[1 - 2E_3(\tau_\nu)]$, where $S_{\nu p}$ is the one-sided spectral flow of equilibrium radiation, $E_3(\tau_\nu)$ is the integral exponent, τ_ν is the optical thickness of plasma. As a result the equilibrium state of the plasma column through which the current, J_1 (MA) $= 0.27(\Lambda/k)^{1/2}$, passes is characterized, according to Afonin (1994), by the values $N_e = 1.26 \times 10^{22} T^{3/2} J_1^2 U_Z / T \exp(U_z/T)$, $r = 0.28 T^{-5/4} [\exp(U_Z/T)/(U_Z/T)]^{1/2}$. If the HP parameters are determined as the equilibrium parameters of this homogeneous cylindrical column, then the expressions found for the radius r (cm) and electron density N_e (cm^{-3}) give HPP parameters sought for.

When interpreting the experimental data (Afonin *et al.*, 1997*a*), it should be noted that at $T \sim 400$–900 eV plasma contains, mainly, H- and He-like ions of aluminum. For this temperature interval it is possible to find $J_1 = 0.20$–0.11 MA, $r = (1$–$10) \times 10^{-4}$ cm, $N_e = (9.3$–$1.1) \times 10^{23}$ cm^{-3} at $Z = 11$, and $J_1 = 0.26$–0.18 MA, $r = (1$–$10) \times 10^{-4}$ cm, $N_e = (1.1$–$22) \times 10^{23}$ cm^{-3} at $Z = 12$. Insofar as current in a pinch J has not exceeded 0.22 MA, it is possible to conclude that the quasi-equilibrium has been already reached at the current being equal to the critical one $J_1 = 0.2$ MA and $T = 400$ eV, at which the transversal size of HPP amounted to ~ 10 μm for He-like ions of aluminum, and $N_e \sim 2.3 \times 10^{23}$ cm^{-3}, which agreed satisfactorily with experimental data.

At $J_1 < J$, where a J-current passes in the pinch, the transversal size of the constriction decreases (both in He-like ions, and in H-like ions), and the temperature and density of plasma are increasing. As is seen from the given estimates, at the same time the drop in the critical current value takes place that is necessary for the quasi-equilibrium mode. However, with ionization of He- and H-like ions of aluminum and the line radiation plasma drop associated with it, the critical current value increases and at $J_1 = J$ the quasi-equilibrium mode becomes possible. But the constriction compression mode can be changed by the quasi-equilibrium mode and scatter in that case as well, if the condition of $J_1 \geq J$ is satisfied. It can be also satisfied if in the process of the constriction evolution the displacement of current from it to the pinch periphery takes place (Sarkisov *et al.*, 1995).

Analogous estimates (Afonin, 1994) show that at 300 eV $< T <$ 800 eV in plasma of iron there are ions with open L-shells. Accordingly, L-size of the HPP equilibrium state amounts to $\sim$3–20 μm. With increasing temperature

https://doi.org/10.1017/S0263034601193018 Published online by Cambridge University Press

the *L*-shell of ions is emptied, and the *K*-shell is excited. At the same time the *K*-size of HPP is estimated to be equal to ~ 7 μm with density $N_e \sim 10^{24}$ cm^{-3}. For plasma of silicon the *L*-size amounts to $d = 10$–30 μm at $T = 200$–300 eV, but the *K*-size to $d < 30$ μm at temperature of *K*-spectra excitement $T > 660$ eV. These estimates also agree satisfactorily with experimental data (Aranchuk *et al.*, 1986).

8. SPONTANEOUS MAGNETIC FIELDS AND HOT PLASMA POINTS MIGRATION

Let the radius of the unperturbed part of the cylindrical plasma column being found in the inherent magnetic field of the current J (A) $= 1.4 \times 10^4 T^{3/4} Z/Z_N^2$ passing through the plasma be R (cm), and r_0 (cm) be the radius of constriction. Assume that in the constriction plasma with the average charge of ions Z, temperature T (eV) $= T_I = T_e$, electron density N_e (cm^{-3}), the equilibrium radius $r_0 = (J^2 Z^{1/2}/T^{11/2} Z_N^{7/2})^{1/3}$, and density $N_e = 10^9 J^{2/3} T^{8/3} Z^2$, where Z_N is the ion nuclear charge, will appear in accordance with Koshelev *et al.* (1991).

In accordance with Eq. (3) and assuming that in the constriction plasma the temperature gradient is perpendicular to the axis, but the density gradients (with regard for plasma flowing out) are directed along it, it is possible to expect the SMF generation. Making use of Eq. (3) for the equilibrium radius, critical current, and its magnetic field, it is possible to obtain an estimate of the characteristic rise time of SMF up to the value of the inherent magnetic field of a current J in the form of τ (ns) $\sim 1.6 \times 10^7 / T^{19/12} Z_N^{5/3}$ at $Z \sim Z_N$, $\nabla N_e \sim N_e/r_0$, $\nabla T \sim T/r_0$. Taking into account that according to Miln-Tompson (1964) the appearance of He-like ions in plasma takes place when $T \sim (2$–$4) \times 10^{-3} Z_N^4$, but Ne-like ions appear at $T \sim 6 \times 10^{-4} Z_N^4$, we shall obtain the estimate $\tau \sim 1$ ns and $\tau \sim 10$ ns for iron plasma with He- and Ne-like ions, respectively. Therefore, SMF can quickly increase up to the value comparable with the magnetic field of the critical current. At the same time, in one part of the constriction SMF weakens the inherent magnetic field of the current J, but intensifies in the other one. There is the unbalance between the plasma pressure and the total magnetic field pressure. It can specify the occurrence of a surface wave that propagates along the plasma column and after this wave plasma is expanded. The estimate of its velocity along the plasma column in which the role of surface tension plays the value $\alpha = (0.2J)^2/8\pi r^2$ in the form of

$$V\,(\mathrm{cm/s}) = 3.16 \times 10^{10} (Z_i J^2 th(\pi/2a))^{1/2}/r_0(\pi aNA)^{1/2}. \quad (6)$$

It is easily possible to obtain (Afonin *et al.*, 1998), if one makes use of the theory of surface waves which has been developed in hydrodynamics (Miln-Tompson, 1964). At the same time, A is the atomic weight of elements, N is the ion density, $a = \lambda/4r_0$ is the aspect ratio, and $\lambda/2$ is the construction length.

In Figure 10 the X-ray photochronogram of an Al-wire explosion that was obtained in one of the experiments at the installation SIGNAL is given.

It is seen that one of the HPPs moves from the cathode to the anode with an average velocity $V \sim 2.5 \times 10^7$ cm/s in ~ 4 ns, while the second one moves in the opposite direction. The motion of HPP can be related to the generation of an SMF in the constriction. At the same time, the HPP migration (from the anode or to the anode) depends on the spatial orientation of the plasma density and temperature gradients in the constriction. In our case, while taking into account the direction of the density gradients along the edges of the constriction, it is necessary to assume the temperature gradient direction in these regions from the plasma axis to the its corona that agrees with the conception on the availability of a cold dense core and a hot rarefied corona. Then from Eq. (6), the estimation of the summary current J in plasma of He-like ions of aluminum $J \sim 3.4 \times 10^5$ A follows at $V = 2.5 \times 10^7$ cm/s and at the characteristic HPP parameters $d = 10^{-3}$ cm, $N_e = 10^{23}$ cm^{-3}. It significantly exceeds the value of current in a pinch $J = 200$ kA being characteristic for the described experiment and can be indicative of the generation in the region of the SMF constriction.

According to Bartnik *et al.* (1991), at the discharge of 200 kA current on the neon jet, the constriction has been registered with $T = 0.2$ keV, $\lambda/2 = 2r_0 = 0.1$ cm, $N_e = 2 \times 10^{19}$ cm^{-3}, which is displaced a distance of 0.7 cm during 50 ns in a direction of the cathode. Using these data as well as the fact that the jet plasma has not been possessed of a cold dense core and after compression and thermalization the temperature gradient is directed in it to the axis, from

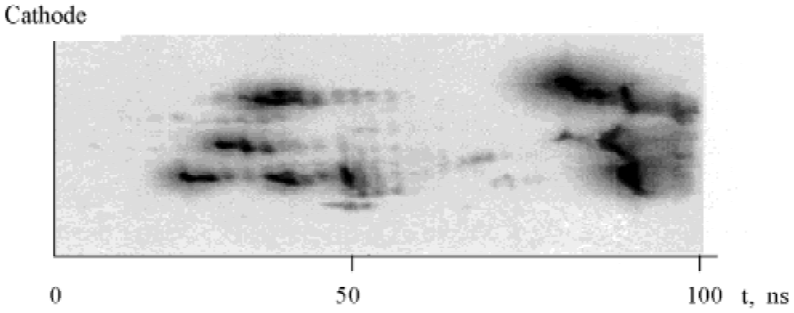

Fig. 10. X-ray photochronogram of the explosion of an Al wire, 8 mm in length.

https://doi.org/10.1017/S0263034601193018 Published online by Cambridge University Press

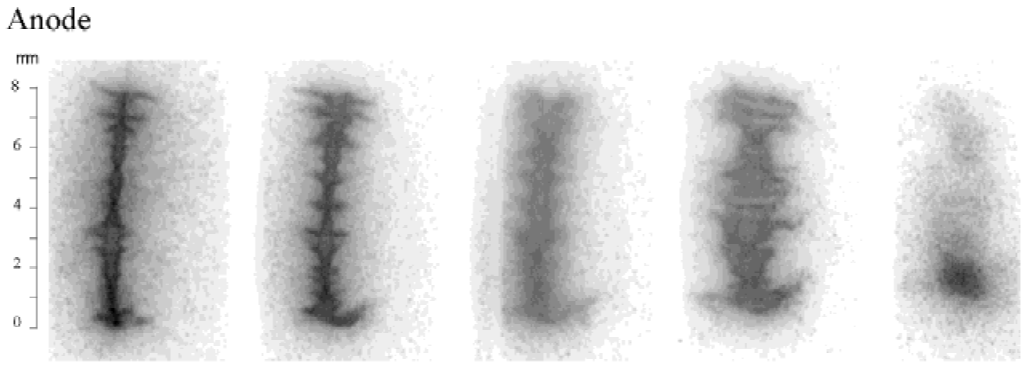

Fig. 11. Successive X-ray images of the load plasma column. The frame duration is 5 ns, and the time intervals between frames are 5 ns. The first frame starts 15 ns after the load current starts to flow. The load is aluminum wire, 21 μm in diameter and 8 mm in length; the maximum current is 160 kA; the current rise time is 60 ns.

Eq. (6) it is possible to find $V = 10^7$ cm/s, that agrees satisfactorily with the experimental value.

9. ABOUT FIXING A HOT POINT OF A PINCH

Derzhiev *et al.* (1986) evaluated the possibility of two ways of fixing a hot point of a *z* pinch in space by introducing perturbations either into the initial shape of the wire (made of homogeneous material) or into the wire material density without changing the shape of the wire. In the latter case, a composed wire with its central part and ends made of different materials is required. The outcome of estimates based on a modified model of a pinch—"a snow plow" (Afonin *et al.*, 1999)—indicate a preference for the second method.

One of the possible versions of the load design for a SIGNAL accelerator is a composite wire made of light and heavy elements (aluminum and, e.g., tungsten). In this case, the length of the Al insert can be chosen according to data (Afonin *et al.*, 1997*b*) on the length of large-scale perturbations ($\sim$ 0.1–0.15 cm), which can give rise to HPP in the *z* pinch of an Al wire, 20 μm in diameter.

Experiments with the purpose of investigating the possibility for fixing HPP in a *z* pinch (Afonin *et al.*, 1998, 1999) were carried out on the high-current SIGNAL generator. We used cylindrical wires, 8 mm in length and 20–25 μm in diameter, as the load. The central part of the wires (1.3–2 mm in length) was made of aluminum or glass, and the ends were made of tungsten.

The frame-by-frame imaging of the 0.1–10 keV X-ray emission from the *z* pinch was performed by a SKhR4 recorder producing 5 frames with exposure times from 3 to 12 ns and time intervals between the frames from 3 to 15 ns (Derzhiev *et al.*, 1986). The time duration of the X-ray emission from the *z* pinch was measured by an RFR4 streak camera, and the frame-by-frame optical images of the plasma column were produced by an SER4 streak camera (Afonin *et al.*, 1999*a*; Afonin & Murigov, 1998). In this series of experiments, the line X-radiation (LXR) was recorded by a spectrograph (Afonin *et al.*, 1997*a*, 1999) with a planar potassium biphthalate crystal and entrance slit. The spectrograph made it possible to detect LXR from H- and He-like Si and Al ions contained in the inserts of exploding tungsten wires as components of quartz filament (SiO_2), aluminum wire (Al), and silicate adhesive (SiO_2). In addition, in this spectral range, we also carried out space resolved measurements of the XR continuum from tungsten ions in the spec-

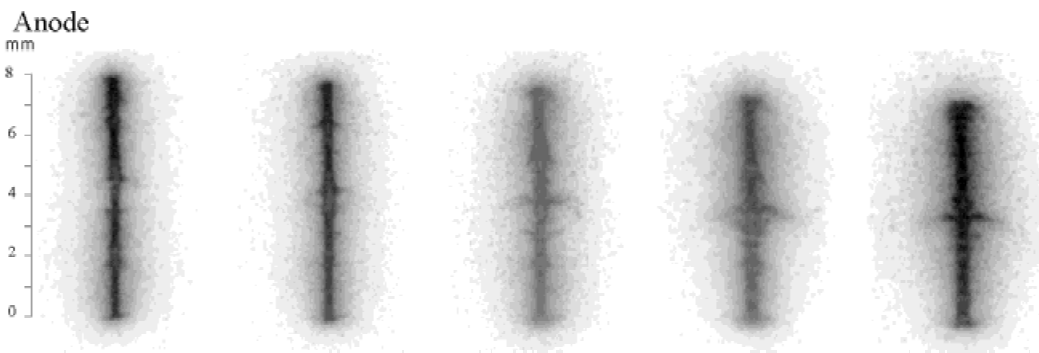

Fig. 12. Successive X-ray images of the load plasma column. The frame duration is 3 ns, and the time intervals between frames are 5 ns. The first frame starts $\sim$20 ns after the load current starts to flow. The load is a composed W-Al-W wire, 20 μm in diameter and 8 mm in length (the length of the Al insert is 1.3 mm); the maximum current is 140 kA; the current rise time is 50 ns.

https://doi.org/10.1017/S0263034601193018 Published online by Cambridge University Press

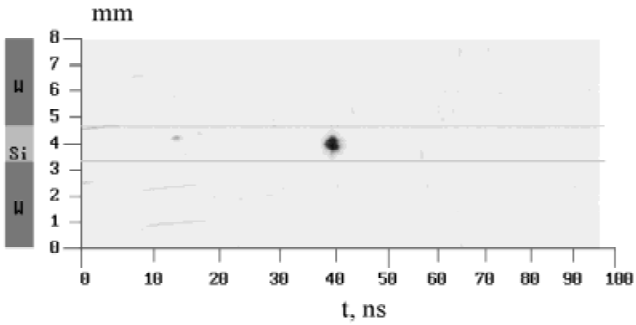

Fig. 13. X-ray streak-camera images of the explosion of a composed W-SiO_2-W wire (a SiO_2 rod, 2 mm in length and 19 μm in diameter, inserted between tungsten wires, 20 μm in diameter). The load length is 8 mm; the maximum current is 150 kA; the current rise time is 60 ns.

trograph sagittal plane. The measurements of LXR of Al and Si ions allow us to determine the electron temperature T_e. From the measurements of LXR of Al ions, we can also determine the plasma mass density ρ and characteristic size of HP in the spectrograph sagittal plane.

Figures 11 and 12 show successive images of the plasma column produced in the explosion of an Al wire, 20 μm in diameter, and a composite W-Al-W load of the same diameter. The images were obtained with an SKhR4 recorder with a set of five pinholes, 30 μm in diameter.

We draw attention to the fact that, in Figures 11 and 12, there are no developed instabilities higher than the constriction mode $m = 0$. The images demonstrate the difference in the character of the explosion of this type of loads: In the case of a uniform Al wire, the appearance and development of many constrictions and radial bulges are seen, whereas, in the case of W-Al-W wire, the radial bulges occur predominantly at the ends of the aluminum insert. These bulges move in opposite directions at velocity of $\sim 10^7$ cm/s; the velocity at which one of the bulges moves from the anode to cathode exceeds the velocity at which the other bulge moves in the opposite direction. Assuming that the density gradients at the constriction edges are directed along the pinch axis and the temperature gradients in these regions are directed from the pinch axis to the corona, we can conclude that the generation of an SMF disturbs the balance between the plasma pressure in the constriction and the total magnetic field pressure. The total magnetic field pressure at the anode edge of the constriction is higher than at the cathode edge. As a result, the constriction edge propagating towards

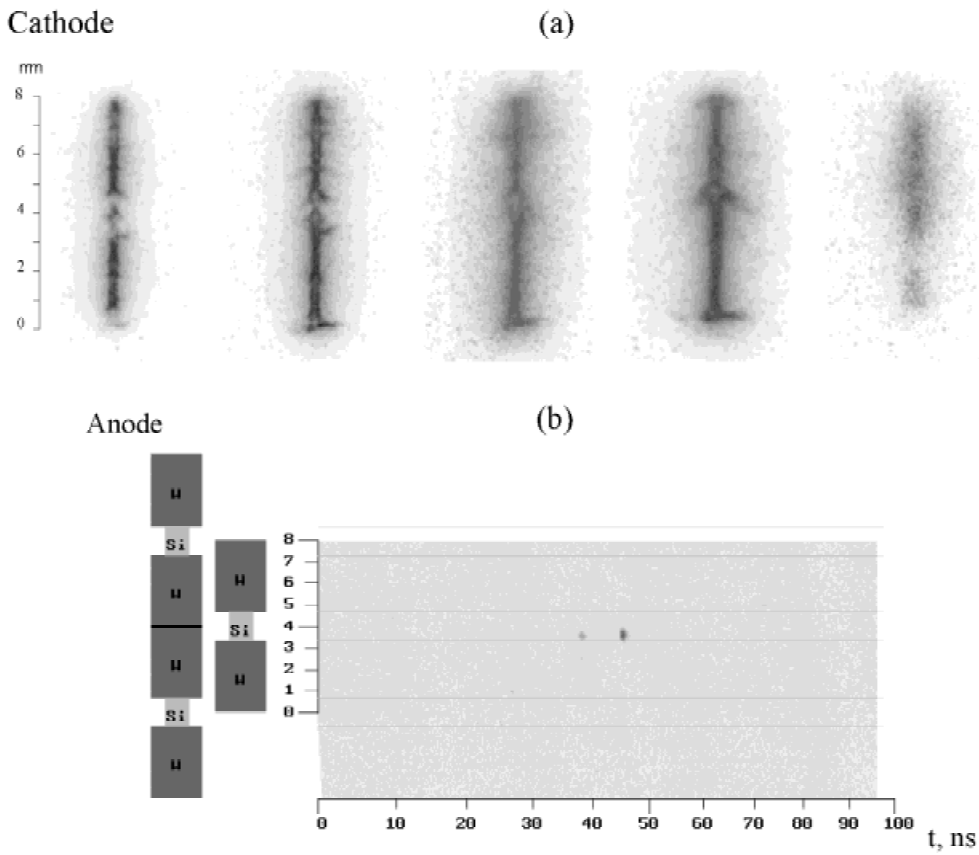

Fig. 14. (a) Successive X-ray images of the load plasma column are shown. The frame duration is 5 ns, and the time intervals between frames are 5 ns. The first frame starts 15 ns after the load current starts to flow. (b) X-ray streak-camera images of the load explosion are shown. The load is an 8-mm-long composed wire (a SiO_2 rod, 2 mm in length and 20 μm in diameter, inserted between tungsten wires, 50 μm in diameter). The maximum current is 180 kA; the current rise time is 100 ns. The vertical scale is in millimeters.

https://doi.org/10.1017/S0263034601193018 Published online by Cambridge University Press

the anode moves with a higher velocity than that propagating toward the cathode.

The generation of an HPP can proceed as follows: The initial shock wave (constriction) in the aluminum plasma arrives at the system axis and forms an HPP. Then, the shock waves that form at the constriction edges propagate in both directions along the pinch axis. When the shock reaches the interface separating the different load materials, it is partially reflected. Converging in the plasma of the insert, they can generate the next HPP, which can be displaced with respect to the previous one. A cumulation of plasma bulges magnifies this effect.

We carried out experiments on the explosion of an 8-mm-long composite wire (an aluminum rod, 1.3 mm in length and 20 μm in diameter, inserted between W wires, 20 μm in diameter); the load current reached ~130 kA at 50 ns. The data obtained indicated that a single HPP was produced at the center of the insert. The plasma mass density in the HPP was ~1 g/cm^3, and the transverse size of HPP was ~0.4 mm. The electron temperature in HPP was ~0.37 keV.

Figure 13 shows a typical X-ray streak-camera image of the explosion of composed W-SiO_2-W filaments. It is seen that a single HPP is produced in the insert. The HPP size along the pinch axis is ~0.5 mm, and its lifetime is ~2 ns.

Figure 14 shows successive X-ray images of plasma column and the X-ray streak-camera image of the electric explosion of a composed wire (a SiO_2 rod, 1.3 mm in length and 21 μm in diameter, inserted between W wires 50 μm in diameter).

This experiment is of particular interest, because, in this case, the initial perturbations were introduced into both the shape and the density of the load. In this experiment, the streak-camera image was obtained with three slit cameras with slit dimensions of 0.1 × 5 mm^2, 0.2 × 5 mm^2, and 0.05 × 5 mm^2. Each camera produced the corresponding pinch image at the photocathode. The streak-camera images

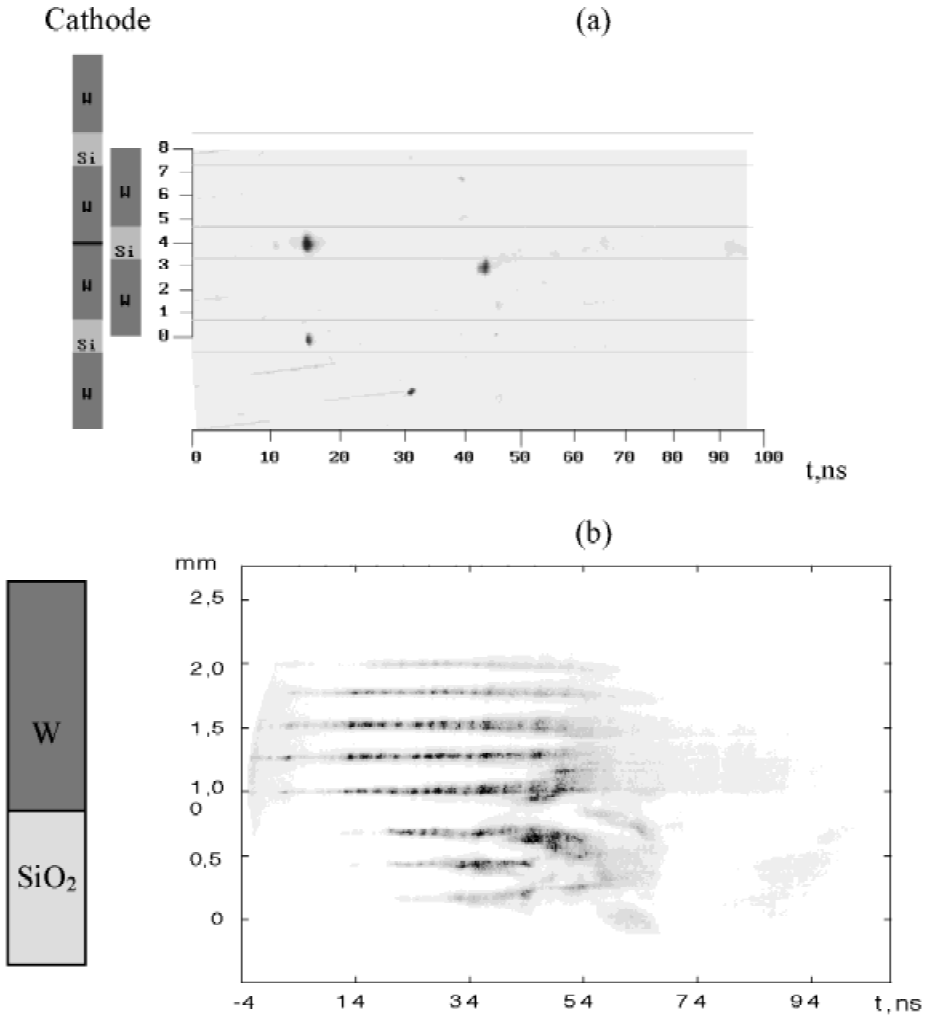

Fig. 15. (a) X-ray and (b) optical streak-camera images of the explosion of an 8-mm-long composite load (a SiO_2 rod, 1.3 mm in length and 19 μm in diameter, inserted between tungsten wires, 20 μm in diameter). The maximum current is 190 kA; the current rise time is 50 ns.

https://doi.org/10.1017/S0263034601193018 Published online by Cambridge University Press

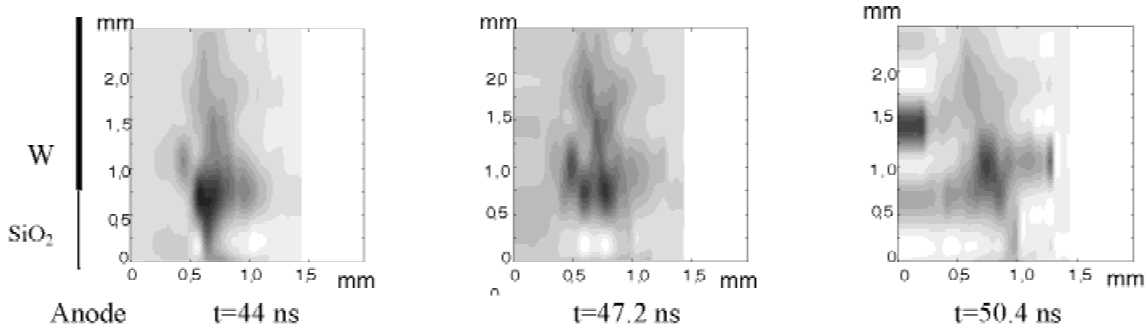

Fig. 16. Reconstructed (from the optical streak-camera images of Fig. 15) successive images of the plasma column of a composed wire.

demonstrate the formation of two HPPs in the plasma of the insert, which are separated in time by a small interval, the HPP size along the pinch axis being <0.3 mm. In turn, the spectral measurements allow us to identify emitting plasma as a silicon plasma with a single HP with the electron temperature 0.38 keV and transverse size of ~ 0.25 mm.

Figure 15 shows X-ray and optical streak-camera images (for eight cross sections of the central region) of the explosion of a composed load (a SiO_2 rod inserted between tungsten wires). (The figure demonstrates the correspondence between the load and its image).

According to the X-ray streak-camera image, in this case, two HPPs are formed in the center and at the insert boundary. The characteristic sizes of HPPs along the system axis are <0.4 mm, and lifetimes ~ 1 ns and 0.5 ns, respectively. At the same time, the spectral measurements indicate the presence of a single HP near the insert boundary. The emission from this HPP is produced by the plasma consisting of the silicon-tungsten mixture. Furthermore, as follows from spectral measurements, there are no HPPs in the tungsten plasma. Therefore, the appearance of an HPP "image" on the streak-camera image can be explained as a defect of the photo film or of its development.

Finally, Figure 16 shows the optical image of the central part of the pinch. This image is reconstructed from the optical streak-camera images of Figure 15.

An HP, which was detected near the gluing point at $t \sim 45$ ns, is also seen in the streak-camera image. From the reconstructed images, the transverse size of the HPP was estimated as equal to 0.25–0.4 mm.

Thus, experimental results indicate that introducing an initial perturbation into the density of the load can control the generation of HPP in a fast *Z*-pinch.

ACKNOWLEDGMENTS

The author expresses thanks to Drs. V.M. Murugov, A.V. Senik, V.P. Lasarchuk, and all the others participating in VNIITF operations on *z* pinches. The author is also sincerely grateful to Prof. V.P. Smirnov for his interest in the work and useful discussions.

REFERENCES

Afonin, V.I. (1994). *Plasma Physics Reports* **20**, 311.
Afonin, V.I. (1995). *Plasma Physics Reports* **21**, 250.
Afonin, V.I. (1999). *Plasma Physics Reports* **25**, 678.
Afonin, V.I. (2000). *Plasma Physics Reports* **26**, 318.
Afonin, V.I. (2001). *Plasma Physics Reports* **27**, 614.
Afonin, V.I. *et al.* (1988*a*). Zababakhin Scientific Talks, Snezhinsk, Russia. Abstracts, p. 79.
Afonin, V.I. *et al.* (1988*b*). Zababakhin Scientific Talks, Snezhinsk, Russia. Abstracts, p. 106.
Afonin, V.I. *et al.* (1996) *Proc. of the 11th Int. Conf. "BEAMS-96"*, Prague, 697.
Afonin, V.I. *et al.* (1997*a*). *Plasma Physics Reports* **23**, 1002.
Afonin, V.I. *et al.* (1997*b*). *Plasma Physics Reports* **23**, 1008.
Afonin, V.I. *et al.* (1998). *Plasma Physics Reports* **24**, 503.
Afonin, V.I. *et al.* (1999). *Plasma Physics Reports* **25**, 792.
Afonin, V.I. & Murugov, V.M. (1998). *Plasma Physics Reports* **24**, 363.
Aivasov, I.K. *et al.* (1985). *Pis'ma Zh. Eksp. Teor. Fiz.* **41**, 111.
Aranchuk, L.E. *et al.* (1986). *Fiz. Plasmy* **12**, 1324.
Aranchuk, L.E. *et al.* (1997). *Plasma Physics Reports* **23**.
Bartnik, A. *et al.* (1990). *Fiz. Plazmy* **16**, 1482.
Bartnik, A. *et al.* (1991). *Methods for Studying Radiative-Collisional Processes in Laser Plasmas* (Skobelev, I.Yu., and Faenov, A.Ya., Eds.), p. 50 Moscow: NPO VNIIFTRI.
Bobrova, N.A. *et al.* (1988). *Fiz. Plasmy* **14**, 1053.
Braginsky, S.I. (1963). *Plasma Theory Questions* (Leontovich, M.A., Ed.), issue 1, p. 183 Moscow: Atomizdat.
Branitsky, A.V. *et al.* (1991). *Fiz. Plasmy* **17**, 531.
Branitsky, A.V. *et al.* (1999). *Plasma Physics Reports* **25**, 1060.
Breton, C. *et al.* (1978). *Quant. Spectrosc. Rad. Transport* **19**, 367.
Derzhiev, V.I. *et al.* (1986). *Ion Radiation in Dense Non-equilibrium Plasmas*. Moscow: Energoatomizdat.
Gus'kov, S.Yu. *et al.* (1998). *Pis'ma Zh. Eksp. Teor. Fiz.* **67**, 531.
Ivanenkov, G.V. *et al.* (1995). *Zh. Tekh. Fiz.* **65**, 40.
Kadomtsev, B.B. (1963). *Plasma Theory Questions* (Leontovich, M.A., Ed.) issue 2, p. 173. Moscow: Atomizdat.
Kalantar, D.H. & Hammer, D.A. (1993). *Phys. Rev. Lett.* **71**, 3806.
Koshelev, K.N. *et al.* (1991). *Multiply Charged Ion Spectroscopy in Hot Plasma* (Safronova, U.N., Ed.) p. 163 Moscow: Nauka.

https://doi.org/10.1017/S0263034601193018 Published online by Cambridge University Press

Lindl, J.D. (1995). *Phys. Plasmas* **2**, 3933.
Miln-Tompson, L.M. (1964). *Theoretical Hydrodynamics*. Moscow: Mir.
Raizer, Yu.P. (1987). *Physics of Gas Discharges*. Moscow: Nauka.
Sarkisov, G.S. *et al.* (1995). *Zh. Eksp. Teor. Fiz.* **108**, 1355.
Vainstein, L.A. *et al.* (1979). *Excitation of Atoms and Spectral Lines Broadening*. Moscow: Nauka.
Velikhov, E.P. *et al.* (1972). USSR DAN **205**, 1328.
Vikharev, V.D. *et al.* (1990). *Fiz. Plazmy* **16**, 379.
Yan'kov, V.V. (1991). *Fiz. Plazmy* **17**, 521.
Zel'dovich, Ya.B. & Raizer, Yu.P. (1967). *Physics of Shock Waves and High-Temperature Hydrodynamic Phenomena*. New York: Academic Press.
Zhdanov, S.K. & Trubnikov, B.A. (1986). *Fiz. Plasmy* **12**, 851.

https://doi.org/10.1017/S0263034601193018 Published online by Cambridge University Press